Deriving microstructure and fluid state within the Icelandic crust from the inversion of tomography data

M. Adelinet,[1,2] C. Dorbath,[3] M. Le Ravalec,[1] J. Fortin,[2] and Y. Guéguen[2]

Received 25 November 2010; revised 23 December 2010; accepted 3 January 2011; published 9 February 2011.

[1] The inversion of seismic data to infer rock microstructural properties and fluid flow patterns in the crust is a challenging issue. In this paper, we develop an effective medium model for estimating velocities in porous media including both pores and cracks and use it to derive the distribution of crack density beneath the Reykjanes Peninsula from accurate tomography data. Outside the active hydrothermal areas, crack density is shown to decrease with depth. There are two main reasons for this: the closure of cracks because of the increasing overburden and the secondary filling of cracks because of hydrothermal flows. However, crack density may locally increase with depth beneath the southwestern part of the Kleifarvatn lake. This is consistent with the presence of a deep reservoir with supercritical fluids under pressure, which may activate hydrofracturing processes. We recognize that capturing the link between seismic data and the physical properties of crust is very difficult. This study shows that a combination of mechanical concepts and effective medium theory contributes to improve our understanding of the phenomena occurring within the Icelandic crust. **Citation:** Adelinet, M., C. Dorbath, M. Le Ravalec, J. Fortin, and Y. Guéguen (2011), Deriving microstructure and fluid state within the Icelandic crust from the inversion of tomography data, *Geophys. Res. Lett.*, *38*, L03305, doi:10.1029/2010GL046304.

1. Introduction

[2] This study focuses on one of the most active regions in Iceland, in terms of seismic and hydrothermal events, the Reykjanes Peninsula, which is located in the southwestern part of the island. This peninsula is the northward prolongation of the Reykjanes oceanic ridge and consists of volcano-tectonic segments. The middle parts of these segments are associated with high temperature hydrothermal phenomena [*Arnorsson*, 1995]. The oceanic crust is about 15–20 km thick beneath the Reykjanes Peninsula [*Foulger et al.*, 2003]. Field observations and geophysical data suggest a coupling between fluid flow and deformation in the upper crust of this particular region [*Vadon and Sigmundsson*, 1997; *Clifton et al.*, 2003; *Geoffroy and Dorbath*, 2008; *Lupi et al.*, 2010]. Our goal is to use effective medium (EM) modeling to investigate the evolution of crack parameters (density and aspect ratio) at depth and also laterally.

[3] Relating seismic data to fluid processes at depth is not straightforward. However, this goal can be achieved when we know how much and where fluid was injected. For instance, *Dorbath et al.* [2009, 2010] showed that seismic response and stress field fully depend on deep massive water injections in Soultz-sous-Forêts (France) within the EGS (Enhanced Geothermal System) project. The context in Iceland is quite different as the quantity and the state of water at depth are unknown. Thus, we developed a model based on the EM theory to characterize the state of the Icelandic crust beneath the Reykjanes Peninsula. EM models have already been applied to explain seismological observations as a function of crack closure with depth [*Tsuji and Iturrino*, 2008]. They also allow characterization of earthquake rupture areas. For instance, *Zhao and Mizuno* [1999] and *Mishra and Zhao* [2003] used the EM model of *O'Connell and Budiansky* [1974] to characterize the hypocenter regions of the Kobe (1995) and Buhj (2001) earthquakes in terms of crack density and saturation rate.

[4] One problem currently tackled in geophysics is the relationship between field studies and model calibration from real data. We propose an original approach coupling both of them. Our objective is to supply an EM model with high-resolution seismic tomography data collected in 2005 on the Reykjanes Peninsula to characterize crust microstructure.

2. Initial Tomography Data

[5] Figure 1 shows the P- and S-waves velocities derived from tomography for the studied area [*Geoffroy and Dorbath*, 2008]. An anomalous zone, called the Kleifarvatn anomaly, is evidenced at 6 km depth. It is associated to a velocity decrease (Table 1) stronger for P-waves (15% at 6 km depth) than for S-waves (4% at 6 km depth). This specific signature is well-known in geophysics of reservoir: it indicates the presence of a gaseous or supercritical fluid [*Jones and Nur*, 1984; *Mari et al.*, 1999]. The collected P- and S-waves tomography data yield local waves velocities $(V_p, V_s)^m$ at three distinct depth levels: 2, 4 and 6 km. Superscript ^{m} stands for measured data.

3. Theoretical Approach

[6] We develop a model relating seismic velocity to crack parameters (density and aspect ratio) and fluid content. It relies on the definition of an EM with spherical pores and randomly oriented spheroidal cracks [*Adelinet et al.*, 2010]. Both inclusion families are saturated with a fluid phase. For simplicity, the Icelandic crust is assumed to be isotropic (at

[1]IFP Énergies Nouvelles, Rueil-Malmaison, France.
[2]Laboratoire de géologie, Ecole normale supérieure, CNRS UMR 8538, Paris, France.
[3]UMR 154, EOST, IRD, Strasbourg, France.

0094-8276/11/2010GL046304

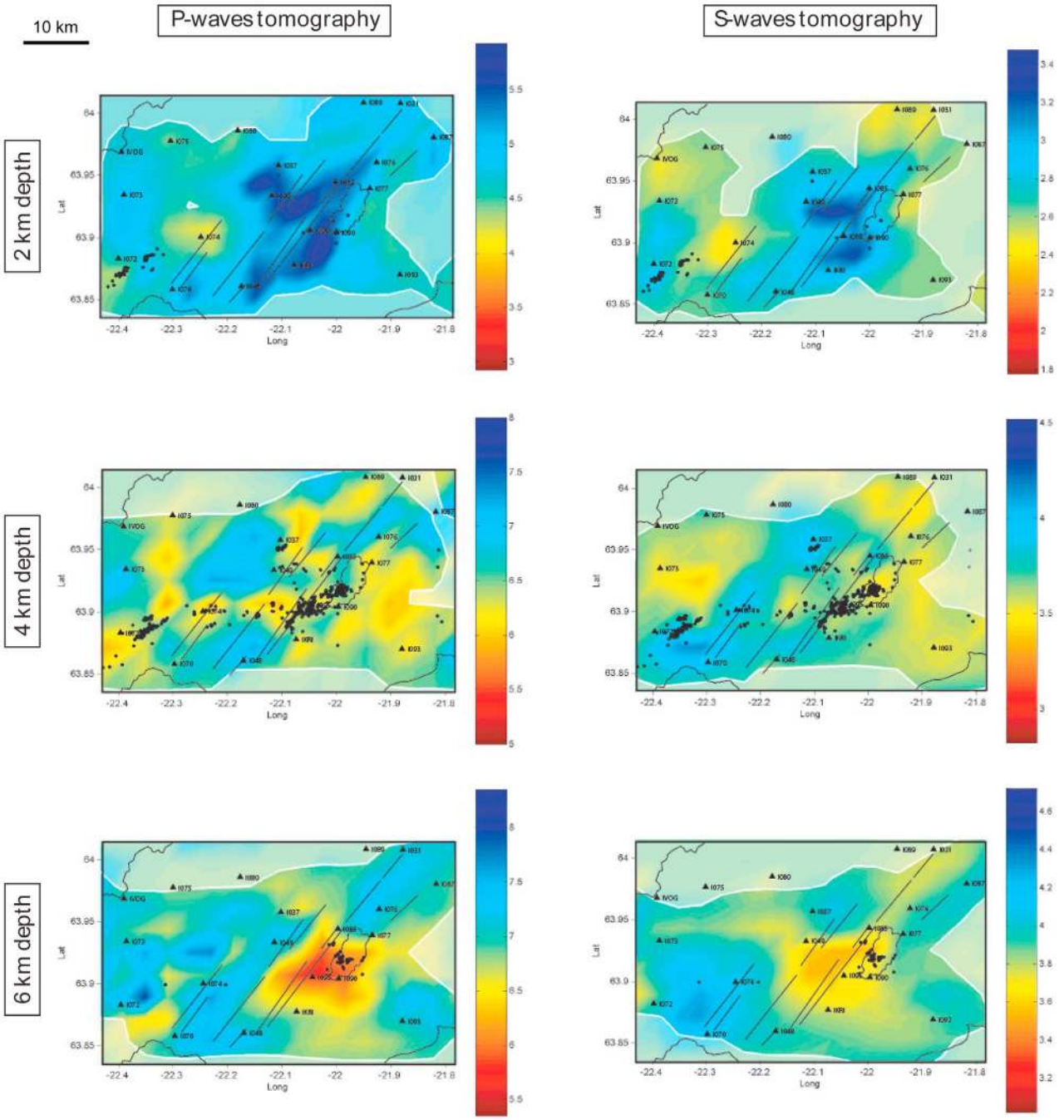

Figure 1. P- and S-waves tomography results for the Reykjanes Peninsula at 2, 4 and 6 km depth. The color bars are centered on the initial model velocity of *Weir et al.* [2001]. The Kleifarvatn lake boundary is drawn. Event locations and surface main fractures are also indicated by filled circles and straight lines, respectively.

least in the first 6 km). We express crack porosity Φ_{cr} as a function of aspect ratio ξ and crack density ρ (equation (1)).

$$\Phi_{cr} = \frac{4}{3}\pi\rho\xi, \tag{1}$$

Crack aspect ratio and density are defined as $\xi = \frac{\omega}{c}$ and $\rho = \frac{1}{V}\sum_i^n c_i^3$ where ω and c are the lengths of the spheroid semi-axes and V the representative elementary volume. In addition, total porosity is assumed to be the sum of two terms: the equant porosity and the crack porosity. The theoretical dry bulk and shear (K_{th}^{dry}, G_{th}^{dry}) moduli for such an effective medium are derived from *Kachanov* [1993] and *Kachanov et al.* [1994] as:

$$\frac{K_0}{K_{th}^{dry}} = 1 + \Phi_p \frac{3(1-\nu_0)}{2(1-2\nu_0)} + \rho\frac{16\left(1-\nu_0^2\right)}{9(1-2\nu_0)}, \tag{2}$$

$$\frac{G_0}{G_{th}^{dry}} = 1 + \Phi_p \frac{15(1-\nu_0)}{7-5\nu_0} + \rho\frac{32(1-\nu_0)(5-\nu_0)}{45(2-\nu_0)}, \tag{3}$$

Table 1. Tomography Data Used in the Local Inversion of the SW Kleifarvatn Area[a]

Depth	$(V_P)^m$	Tomography P-Anomaly	$(V_S)^m$	Tomography S-Anomaly
2 km	5661	+20%	3113	+23%
4 km	6197	−6%	3618	−3%
6 km	5768	−15%	3739	−4%

[a]Velocities are given in m.s^{-1}. Anomalies are calculated from the initial velocity model of *Weir et al.* [2001].

where K_0, G_0 and ν_0 are the bulk modulus, the shear modulus and the Poisson ratio of the free-crack matrix, respectively. Φ_p the equant porosity.

[7] We assume that maximal velocities for each depth level characterize the uncracked crust as suggested by *Zhao and Mizuno* [1999]. Therefore, these maximal values yield estimates of K_0, G_0, and ν_0 for each depth level considered. Then theoretical saturated moduli (K_{th}, G_{th}) are derived from equations (2) and (3) and from Biot-Gassmann's equations [*Gassmann*, 1951]:

$$\begin{cases} K_{th} = K_{th}^{dry} + \frac{\beta^2 K_f}{\Phi + (\beta - \Phi)\frac{K_f}{K_0}} \\ G_{th} = G_{th}^{dry} \end{cases} \quad (4)$$

where Φ is the total porosity, β a dimensionless coefficient defined by $\beta = 1 - \frac{K_{th}^{dry}}{K_0}$ and K_f the fluid bulk modulus. This last parameter strongly varies depending on the saturating fluid phase. Last, we estimate the theoretical P- and S-waves velocities $(V_p, V_s)_{th}$ from $(V_p)_{th} = \left(\frac{K_{th} + \frac{4}{3}G_{th}}{\mu}\right)^{1/2}$ and $(V_s)_{th} = \left(\frac{G_{th}}{\mu}\right)^{1/2}$. Density μ is set to 2700 kg.m^{-3}.

[8] To estimate the state of the fluid at depth, we consider that the saturating fluid is a mixture of a liquid phase with a bulk modulus K_f^{liq} of 2.10^9 Pa and a supercritical phase with a bulk modulus K_f^{SC} of 2.10^8 Pa. There are at least two pieces of evidence supporting this assumption. First, according to log data [*Fridleifsson and Richter*, 2010], depth of the transition from liquid to supercritical phase is around 4 km. Second, the pressure and temperature conditions at depth do not allow the presence of gas. We introduce the liquid ratio R, which varies from 0 (no liquid, only supercritical phase) to 1 (only liquid). In such conditions, the global fluid modulus K_f^{all} is calculated using the Reuss average [*Mavko et al.*, 1998; *Simm*, 2007]:

$$\frac{1}{K_f^{all}} = \frac{R}{K_f^{liq}} + \frac{1-R}{K_f^{SC}}, \quad (5)$$

Now, we define an objective function J, which quantifies the data mismatch in a least square sense. It is used to compare the theoretical velocities and the measured tomography velocities:

$$J(p) = \frac{1}{2}\left[\left(V_P^m - V_P^{th}(p)\right)^2 + \left(V_S^m - V_S^{th}(p)\right)^2\right], \quad (6)$$

The superscripts ^{m} and th refer to the measured data and to the corresponding numerical responses, respectively. Vector p consists of the unknown parameters. It encompasses the crack density ρ, the crack aspect ratio ξ and the liquid ratio R. Then, we minimize the objective function J by adjusting the unknown parameters. In other words, we aim to determine the values of ρ, ξ and R yielding the P- and S-wave velocity values closest to the measured tomography velocities. Minimization is performed on the basis of a trust region algorithm with bound constraints.

4. Numerical Inversion Results

4.1. Crack Density Evolution

[9] In this paragraph, we focus on the evolution of crack density with depth. A preliminary step is the calibration of porosity for each depth level: we performed a few simulations with different porosity values. We eventually selected two sets of porosity data resulting in small J values: (1) at 2 km depth, total porosity is set to 5% (consistent with laboratory data measured on outcrop basalt samples [*Fortin et al.*, 2010]) while (2) at 6 km depth, it is set to 2%. We proceeded as explained above to determine ρ, ξ and R minimizing objective function J. Figure 2 presents the results obtained for crack density. We distinguish two regions in Figure 2: a central zone (including the Kleifarvatn anomaly) and a peripheral one. The central part is characterized by a low crack density at 2 km depth (<0.2) and an increasing one at 6 km depth (>0.4). On the other hand, the peripheral area is attributed a high crack density in subsurface (>0.3) and a very low crack density at depth (<0.15). The general drop of crack density with depth may be related to two causes. First, confining pressure increases because of the increasing overburden weight: this can induce crack closure. Second, high geothermal gradients were observed in the area

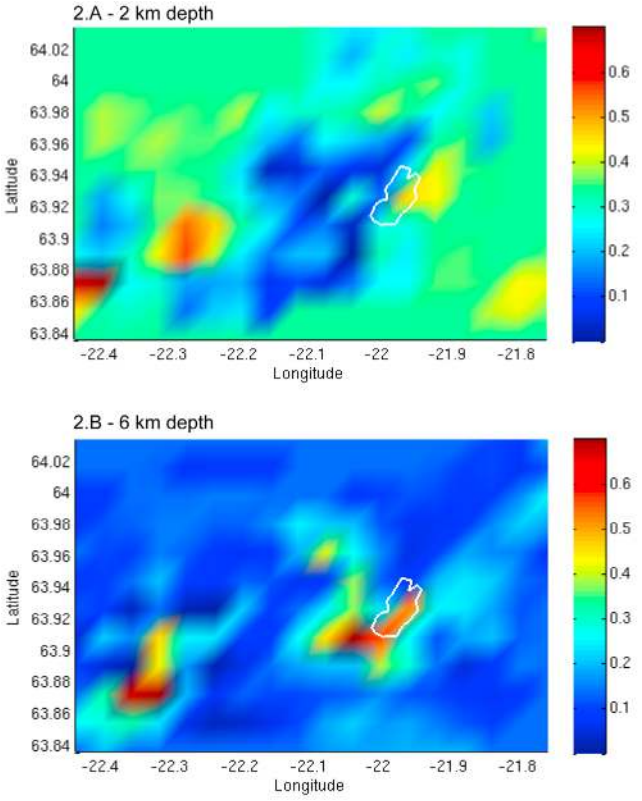

Figure 2. Crack density beneath a part of the Reykjanes Peninsula at (top) 2 and (bottom) 6 depth. The Kleifarvatn lake boundary is drawn in white.

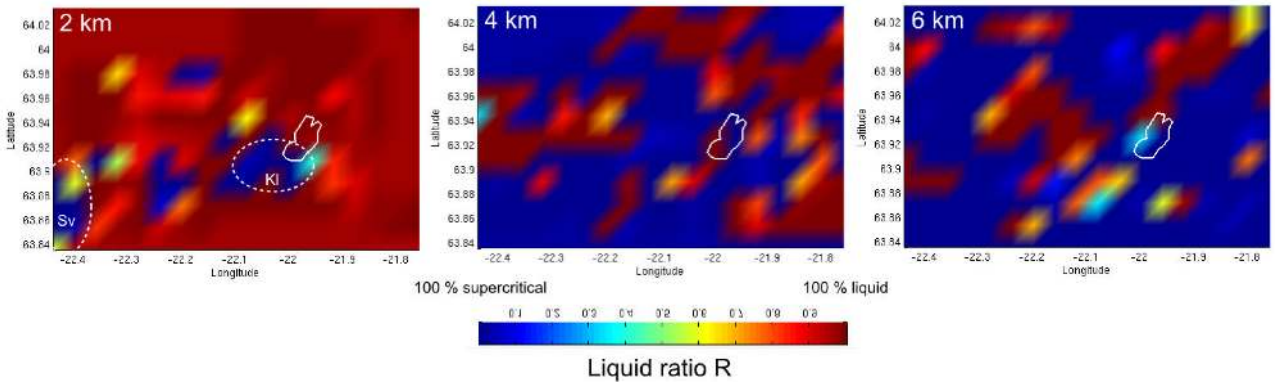

Figure 3. Liquid phase ratio R at 2, 4 and 6 km depth beneath the Reykjanes Peninsula. The dashed ellipses correspond to the surface location of two of the main active hydrothermal systems identified in the Reyjanes Peninsula: Svartsengi (Sv) and Kleifarvatn (Kl) areas.

of interest [*Fridleifsson and Elders*, 2005]: cracks can be filled with secondary precipitation phases resulting from hydrothermal interactions between fluids and rock. In this area, the shallow Icelandic crust contains a dense crack network, which significantly contributes to the drainage of fluids from major surface faults to the deeper crust.

4.2. Fluid State Versus Depth and Consequences on Crack Parameters

[10] Figure 3 shows the variations in R with depth. Our results stress that at 2 km depth, most of the Icelandic crust is saturated with a liquid phase whereas at 6 km depth, most of the deeper crust is saturated with supercritical phase. At 2 km depth, widespread supercritical patches can also be clearly identified. They tend to correspond to the most active surface zones from the hydrothermal point of view. For instance, the areas of Svarstsengi (Sv) and Kleifarvartn (Kl) are known for their important hydrothermal activity on the surface.

[11] To better capture the fundamental role of fluid compressibility, we decided to invert only the (V_p, V_s) couple measured inside the Kleifarvatn anomaly. Figure 4 presents the evolution of crack parameters versus K_f for the three investigated depth levels (colored curves). We chose to vary K_f within a large interval: from 10^6 Pa (gas) to 10^{10} Pa (same order than rock frame). Figure 4 shows that results obtained at 2 and 4 km depth are similar. Furthermore, regardless of fluid compressibility, crack density increases locally with depth. In the same time, aspect ratio decreases of about one order of magnitude, from about 5.10^{-1} at 2 km to less than 10^{-2} at 6 km. We observe that crack density increases drastically for K_f values above a threshold (around 10^9 Pa), especially for 6 km depth. This involves that the flatter the cracks the more sensitive to fluid compressibility. A small variation in K_f is able to induce a significant increase in crack density.

5. Conclusion

[12] In this paper, we show how an effective medium modeling can be used to invert the P- and S-waves velocities derived from tomography for the Reykjanes Peninsula. This makes it possible to detect the presence of a supercritical reservoir at depth beneath the Kleifarvatn anomaly. This result is consistent with the temperature data extrapolated from logs [*Fridleifsson and Richter*, 2010]. This supercritical reservoir is probably overpressurized, which would induce hydraulic fracturing at 6 km depth. Such a phenomenon would explain the local increase in crack density pointed out by our inversion results.

[13] In addition, the fluids within the Reykjanes peninsula crust may originate from meteoric and oceanic water. As a

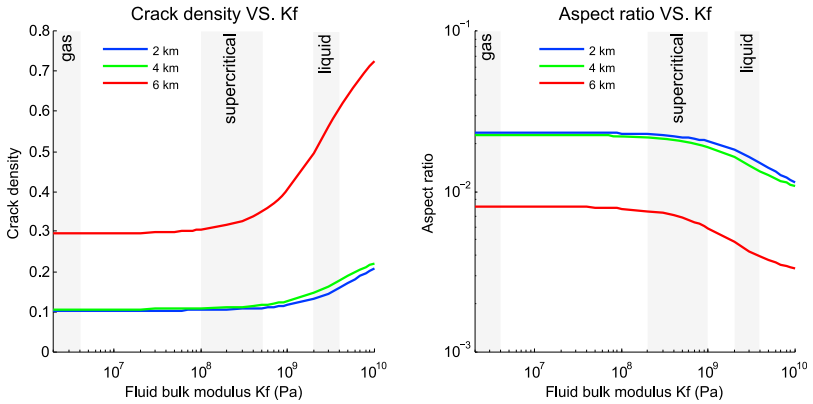

Figure 4. Influence of the fluid bulk modulus on crack parameters. Total porosity is set to 5%. Blue, green and red curves correspond to simulations performed at 2, 4 and 6 km depth, respectively.

result, it can lead to brine phases at depth, which can interact with rocks. Secondary minerals are then formed: they fill up the pore spaces and induce a decrease in crack density and crack aspect ratio in the deeper Iceland crust.

[14] Finally, we have shown that elastic wave velocities recorded at large scale can be processed as local variations in microstructure and fluid state. Effective medium modeling appears to be very useful to constrain such field data and provides efficient tools to invert the seismic responses of a reservoir.

References

Adelinet, M., J. Fortin, and Y. Guéguen (2010), Dispersion of elastic moduli in a porous-cracked rock: Theoretical predictions for squirt-flow, *Tectonophysics*, doi:10.1016/j.tecto.2010.10.012.

Arnorsson, S. (1995), Geothermal systems in Iceland: Structure and conceptual models—I. high-temperature areas, *Geothermics*, *24*, 561–602.

Clifton, A. E., C. Pagli, J. F. Jónsdóttir, K. Eythorsdottir, and K. Vogfjord (2003), Surface effects of triggered fault slip on Reykjanes Peninsula, SW Iceland, *Tectonophysics*, *369*, 145–154.

Dorbath, L., N. Cuenot, A. Genter, and M. Frogneux (2009), Seismic response of the fractured and faulted granite of Soultz-sous-Forêts (France) to 5 km deep massive water injections, *Geophys. J. Int.*, *177*, 653–675.

Dorbath, L., K. Evans, N. Cuenot, B. Valley, and J. Charléty (2010), The stress field at soultz-sous-forêts from focal mechanisms of induced seismic events: Cases of the well GPK2 and GPK3, *C. R. Geosci.*, *342*, 600–606.

Fortin, J., S. Stanchits, S. Vinciguerra, and Y. Guéguen (2010), Influence of thermal and mechanical cracks on permeability and elastic wave velocities in a basalt from Mt. Etna volcano subjected to elevated pressure, *Tectonophysics*, doi:10.1016/j.tecto.2010.09.028.

Foulger, G. R., Z. Du, and B. R. Julian (2003), Icelandic-type crust, *Geophys. J. Int.*, *155*, 567–590.

Fridleifsson, G., and W. Elders (2005), The Iceland Deep Drilling Project: A search for deep unconventional geothermal resources, *Geothermics*, *34*, 269–285.

Fridleifsson, G., and B. Richter (2010), 3D model of fracture zones at Soultz-sous-Forêts based on geological data, image logs, induced microseismicity and vertical seismic profiles, *C. R. Geosci.*, *342*, 531–545.

Gassmann, F. (1951), Uber die elasticizät poröser medien, *Vierteljahrsachr. Naturforsch. Ges. Zurich*, *96*, 1–23.

Geoffroy, L., and C. Dorbath (2008), Deep downward fluid percolation driven by localized crust dilatation in Iceland, *Geophys. Res. Lett.*, *35*, L17302, doi:10.1029/2008GL034514.

Jones, T. D., and A. Nur (1984), The Nature of seismic reflections from deep crustal fault zones, *J. Geophys. Res.*, *89*, 3153–3171.

Kachanov, M. (1993), Elastic solids with many cracks and related problems, *Adv. Appl. Mech.*, *30*, 259–445.

Kachanov, M., I. Tsukrov, and B. Shafiro (1994), Effective moduli of solids with cavities of various shapes, *Appl. Mech. Rev.*, *47*, 151–174.

Lupi, M., S. Geiger, and C. M. Graham (2010), Hydrothermal fluid flow within a tectonically active rift-ridge transform junction: Tjörnes Fracture Zone, Iceland, *J. Geophys. Res.*, *115*, B05104, doi:10.1029/2009JB006640.

Mari, J., G. Arens, D. Chapellier, and P. Gaudiani (1999), *Geophysics of Reservoir and Civil Engineering*, Inst. Fr. Pet., Paris.

Mavko, G., T. Mukerji, and J. Dvorkin (1998), *The Rock Physics Handbook*, Cambridge Univ. Press, Cambridge, U. K.

Mishra, O., and D. Zhao (2003), Crack density, saturation rate and porosity at the 2001 Bhuj, India, earthquake hypocenter: A fluid-driven earthquake?, *Earth Planet. Sci. Lett.*, *212*, 393–405.

O'Connell, R. J., and B. Budiansky (1974), Seismic velocities in dry and saturated cracked solids, *J. Geophys. Res.*, *79*, 5412–5426.

Simm, R. (2007), Practical Gassmann fluid substitution in sand/shale sequences, *First Break*, *25*, 61–68.

Tsuji, T., and G. Iturrino (2008), Velocity-porosity relationships in oceanic basalt from eastern flank of the Juan de Fuca Ridge: The effect of crack closure on seismic velocity, *Explor. Geophys.*, *39*, 41–51.

Vadon, H., and F. Sigmundsson (1997), Crustal deformation from 1992 to 1995 at the Mid-Atlantic Ridge, southwest Iceland, mapped by satellite radar interferometry, *Science*, *275*, 194–197.

Weir, N. R. W., R. S. White, B. Brandsdóttir, P. Einarsson, H. Shimamura, H. Shiobara, and R. F. Team (2001), Crustal structure of the northern Reykjanes Ridge and Reykjanes Peninsula, southwest Iceland, *J. Geophys. Res.*, *106*, 6347–6368.

Zhao, D., and T. Mizuno (1999), Crack density and saturation rate in the 1995 Kobe Earthquake Region, *Geophys. Res. Lett.*, *26*, 3213–3216.

M. Adelinet and M. Le Ravalec, IFP Énergies Nouvelles, 1-4 avenue de Bois-Préau, F-92852 Rueil-Malmaison CEDEX, France. (mathilde.adelinet@ifpenergiesnouvelles.fr)

C. Dorbath, UMR 154, EOST, IRD, 5, rue Rene Descartes, F-67084 Strasbourg CEDEX, France.

J. Fortin and Y. Guéguen, Laboratoire de géologie, Ecole normale supérieure, CNRS UMR 8538, 24 rue Lhomond, 75005 Paris France.